Boundary layer noise
Part 1: generation mechanisms

Roberto Camussi, and Alessandro Di Marco
Universitá Roma Tre,
Dipartimento di Ingegneria Meccanica e Industriale,
Via della Vasca Navale 79, 00146, Roma, Italy

Abstract Boundary layer noise concerns the generation of acoustic waves as an effect of the interaction of a fluid with a moving surface. Several issues are related to the noise generation mechanisms in such a configuration. In the present description we focalize mainly onto the case of an infinite flat plate and two main distinct situations are considered. The first one deals with the prediction of the far field noise as accomplished from the classical integral theories, and the main formulations, including Curle's approach, are briefly reviewed. A novel approach based on the computation of the surface transpiration velocity is also presented. The second aspect concerns the interior noise problem and it is treated from the view point of the fluid dynamic effects rather than from that of the structural dynamics. Attention is focused on the statistical properties of the wall pressure fluctuations and a review of the most effective theoretical models predicting statistical quantities is given. The discussion is completed by a short review of the pressure behavior in realistic situations, including the separated boundary layers in incompressible and compressible conditions and the effect of shock waves at transonic Mach numbers.

1 Introduction

Aerodynamic noise from a turbulent boundary layer is a fundamental topic in flow-induced noise and is of interest for both fundamental studies and applied research. The action of the pressure fluctuations indeed provides the driving force to excite surface vibrations and produce acoustic radiation. Many engineering problems are connected with this topic. Fatigue loading on panels of an aircraft fuselage and the vibrational generation of acoustic radiation into an aircraft cabin enclosed by the boundary surface,

R. Camussi (Ed.), *Noise Sources in Turbulent Shear Flows: Fundamentals and Applications*, CISM International Centre for Mechanical Sciences, DOI 10.1007/978-3-7091-1458-2_6,

are two examples among many. Generally speaking, in high speed transport technology, the understanding of the physical mechanisms underlying the generation of pressure fluctuations at the wall, has received increasing attention in view of the use of lightweight and flexible structures. In the field of aerospace launch vehicles design, this problem is of great relevance since vibrations induced in the interior can cause costly damages to the payload while panel vibrations of the external surface must be avoided to prevent fatigue problems and structural damages. In the context of marine transportation, this topic has become quite important in the case e.g. of high-speed ships for passenger transportation where requirements of on board comfort have to be satisfied. This concern has become of great importance for ground transportation as well, notably for high speed trains design. In this case, the effect of pressure fluctuations induced by flow separations (e.g. due to the pantograph cavity) becomes the dominant noise producing mechanism, this situation being of relevance in the automotive industry in general, since large flow separations are unavoidable on cars.

The vibration of a panel induced by a random pressure load leads to acoustic radiation into the flow as well. Also this problem is of relevance for many engineering applications including, for example, the generation of noise from piping systems or the transmission of pressure waves by underwater vehicles, the so–called acoustic–signature.

Due to its importance, since the early 1960s, researchers have been studying this subject using different approaches including experimental investigations, numerical simulations and theoretical speculations.

When a solid surface is overflown by a turbulent boundary layer, several relevant mechanisms contributing to the generation of sound waves, can be identified. To simplify the description, consider the case of a panel subject to a flow on one side. The pressure field on the surface flow side consists of the sum of the turbulence pressures which would be observed on a rigid wall and the acoustic pressures which would be generated by the plane motion in the absence of turbulence. At a first approximation, these two effects can be studied separately. This idea represents the so-called *w*eak coupling approximation and can be derived from an acoustic analogy analysis of the problem [see e.g. Dowling (1983) and Howe (1992)]. The hypothesis that the basic turbulence structure is unaffected by the acoustic motions is indeed the basis of the acoustic analogies and can be accepted if the acoustic velocities are small in comparison with the turbulence velocities. This position, even though not always satisfied, has become accepted as a standard method even at supersonic flow speed [see also Graham (1997)]. The main reason for this is that fully coupled computations are, at present, prohibitive for any length scale of practical relevance even with the most

powerful computer resources. On the other hand, the engineering design still nowadays requires simple models which allows fast understanding and rapid computations.

In view of such considerations, in the following discussions the wall can be considered as a rigid plate and the panel vibrations considered apart.

The problem of the boundary layer noise can then be treated considering two different aspects, namely the so-called *community* noise and the *interior* noise. The first term applies to the effect of the acoustic waves generated by the wall turbulence and evolving in the far field from the flow side of the surface. The second one pertains with the transmission of noise at the side of the surface in still air. In both cases, the attempt to predict the noise emission is based on the correct representation, in a statistical sense, of the random load acting on the surface. For this reason, most of the discussions that follow are concerned with the clarification of the properties of the wall pressure field and the predictability of its main statistical properties. In Figure 1 an overall view of the mechanisms generating sound waves including the definitions adopted therein is reported. Figure 2 evidences the topics faced in the present chapter. The problem related to the interior noise is treated in more details in the second part of this chapter where the theoretical background regarding the noise transmission trough solid structures is presented.

2 The community noise problem

With the term 'Community noise' we mean the far field noise generated at the flow side of a plate moving in a still fluid. Even though very difficult, several theoretical studies have been carried out with the aim of predicting the features of the pressure field radiated by a plane turbulent boundary layer. This topic was first investigated by Curle (1955) and Powell (1960a) using Lighthill's analogy [Lighthill (1952)]. In the following, the integral formulations underlying those original approaches are briefly reviewed along with order of magnitude considerations to establish the importance of the radiative effects.

2.1 Integral formulations

The prediction of the propagation of acoustic waves in the far-field can be attained through an acoustic analogy approach and the search for a solution of the propagation equation derived therein. The reference theory is that of Lighthill (1952) that is based on the rearrangement of the Navier-Stokes equations to form an exact, inhomogeneous, wave equation, whose

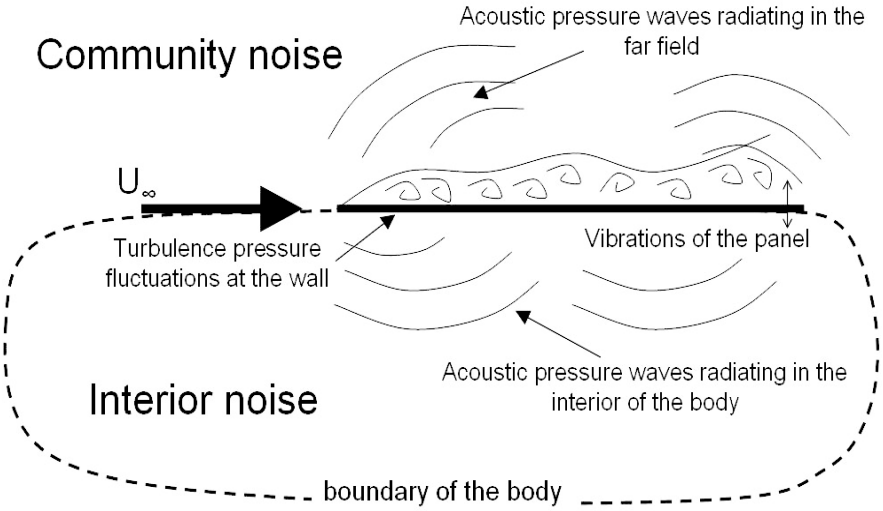

Figure 1. A scheme of the overall mechanisms generating sound waves from a turbulent boundary layer overflowing an elastic flat plate.

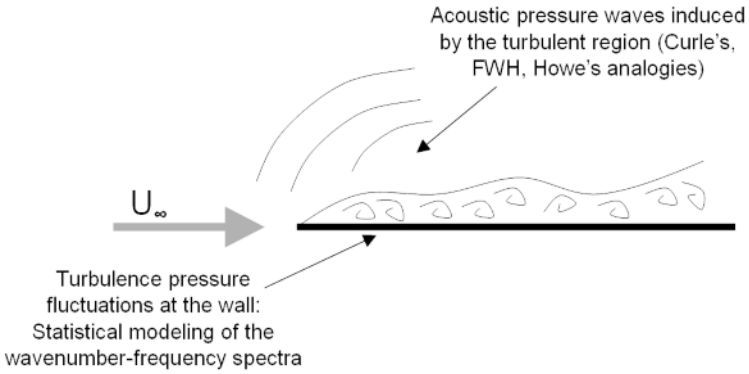

Figure 2. A scheme of the theoretical problems faced in the present chapter.

source terms are significant in the neighborhood of vortical regions of the flow. As pointed out above, the sound is supposed to be a sufficiently small component of the whole motion that its effect on the main flow can be neglected. This hypothesis can be accepted in low Mach number (M) flows as well as in the absence of resonating systems and multiphase flows.

Detailed discussion about such an approach, elucidating also the applicability limits, are given in other chapters of the present book. Here we limit ourselves to recall the final form of Lighthill's equation that can be written as:

$$\frac{\partial^2 \rho}{\partial t^2} - c^2 \nabla^2 \rho = \frac{\partial^2 T_{ij}}{\partial x_i \partial x_j} \tag{1}$$

where T_{ij} represents the Lighthill stress tensor that, neglecting the viscous terms, is denoted as follows:

$$T_{ij} = \rho u_i u_j + (p - \rho c^2)\delta_{ij} \tag{2}$$

Here, c is the speed of sound, ρ and p are density and pressure perturbations, $\mathbf{u}$ the fluid velocity, $\mathbf{x}$ the spatial coordinate and t the time. This equation is valid within and without a source region. Where linear acoustics is valid, the acoustic pressure can be found from the relation $p = c^2\rho$.

In the presence of solid boundaries, an integral solution of Eq. 1 is based on the introduction of a closed control surface S that may coincide with the surface of a moving body or mark a convenient interface between fluid regions of widely differing mean properties. When S coincides with the solid boundary, the solution of the equation is carried out by imposing suitable boundary conditions on it. The oldest strategy proposed to solve the propagation equation relies on the use of a proper Green's function obtained as a solution of Eq. 1 when the source term is replaced by the impulse point source. The most general representation of this kind is due to Ffowcs Williams & Hawkings (1969), and is applicable to a control surface in arbitrary motion. This equation is obtained by deriving a wave type equation similar to that by Lighthill for a region made up of two subregions bounded by the control surface S. The region inside S contains fluid and/or solid boundaries, the region outside contains only fluid.

Without entering into the details, the integral form of the Ffowcs Williams and Hawkings equation can be obtained again making use of the free space Green's function, leading to the outgoing wave solution. To the purpose of the present discussion, we can consider the case of a stationary control surface, leading the FWH equation to reduce to a simpler formula [see also

Howe (1998)] that was given previously by Curle (1955) and that we report in the following[1]:

$$p(\mathbf{x},t) = \frac{\partial^2}{\partial x_i \partial x_j}\int_V T_{ij}\frac{d^3\mathbf{y}}{4\pi\,|\mathbf{x}-\mathbf{y}|} - \frac{\partial}{\partial x_i}\int\int_S (\rho u_i u_j + p\delta_{ij} - \sigma_{ij})\frac{dS_j(\mathbf{y})}{4\pi\,|\mathbf{x}-\mathbf{y}|} + \frac{\partial}{\partial t}\int\int_S (\rho u_j)\frac{dS_j(\mathbf{y})}{4\pi\,|\mathbf{x}-\mathbf{y}|} \tag{3}$$

As indicated by Howe (1998), Curle's equation written for a rigid surface can be used to determine the order of magnitude of the sound generated by an acoustically compact body within a turbulent flow (e.g. a cylinder or an airfoil moving in an incompressible flow). This analysis applies also for non-compact bodies when turbulence interacts with compact structural elements, such as surface discontinuities, edges, corners.

The contribution from the quadrupole volume integral in Eq. 3 to the acoustic power Π radiated in the far field, can be estimated to be

$$\Pi \propto v^3\, M^5 \tag{4}$$

The quadrupole effect predicted by Eq. 4 is the same as in the absence of the body (it is the famous Lighthill's 'eight power' law). On the other hand, at low M, the total power radiated by the dipole term (the first surface integral of equation 3) can be estimated to be:

$$\Pi \propto v^3\, M^3 \tag{5}$$

thus exceeding the quadrupole power by a factor $\sim 1/M^2 >> 1$. The conclusion is that at low M the dipole term is largely dominant. This is the reason why surfaces with disconuities (such as sharp edges, steps, cavities) are much more noisy than smooth walls.

A different conclusion can be driven in the case of non-compact structures, that is, for objects whose size is not small compared to the acoustic wavelength, as is the case of an infinite rigid plate. Curle's approach can again be used, and the presence of the infinite surface can be taken into account by introducing image vortices [Powell (1960b)]. Powell suggests

[1] The notation evidencing the retarded time is not reported for clarity. Interested readers can find a more detailed presentation of this equation and of its theoretical framework in Chapters 1 and 2.

to use a Green's function that is basically obtained by superimposing the free-space G with its image. In this way Powell shows that the pressure exerted on a plane boundary is the result of reflections of the quadrupole generators of the flow itself. In other words it is demonstrated that the surface integral is not a true dipole source but it represents the effect of image quadrupoles. Therefore, as concluded by Howe [Howe (1998)], the apparently strong contribution from the surface pressure dipoles actually reduces to a term of quadrupole strength, thus much less efficient, at low M, in terms of radiated pressure power. In the airframe noise context, if the effect of panel vibrations is not accounted for, it is reasonable to ignore the pure quadrupole radiation from the boundary layers, in comparison with that from edges and other inhomogeinities, such as wing trailing edge, flap side-edges, undercarriage gears and cavities. This is proven even for aircraft of large dimensions. As an example, the noise from the fuselage is expected to be more than 10dB below the level of the trailing edge noise.

However [Hubbard (1991)] the far field acoustic radiation due to panel vibrations might be a significant source of airframe noise in real (full-scale) aircraft. Furthermore [Howe (1998)] the presence of roughness breaks the Powell cancellation mechanism thus leading the dipole contribution to become relevant.

It should be pointed out that some recent numerical experiments [Hu, Morfey & Sandham (2002), Hu, Morfey & Sandham (2003) and Shariff & Wang (2005)] have focused on the role of the wall shear stress, rather than pressure, as sound source. They have shown that unsteady shear stresses can be an efficient sound source of dipole type that can be dominant at low Mach numbers and at very low frequencies.

We refer the reader to classical textbooks [such as Howe (1998)] and to the notes of the other authors included in this book, for further details on the integral approaches.

2.2 Prediction of the far field pressure spectrum: a novel approach

In a recent paper Morino, Leotardi & Camussi (2010) proposed a novel approach for estimating the far field pressure Power Spectrum (PSD) by the knowledge of the PSD of the pressure on the boundary surface, provided that the region where the flow is rotational and/or nonlinear is adequately thin. In order to accomplish this, the PSD of the pressure at any given point (either in the field or on the boundary) is evaluated in terms of the Power Spectral Density (PSD) of the transpiration velocity over the boundary surface. This contribution is denoted as given by *equivalent sources* χ_B.

The approach briefly described therein is based upon a formulation that falls within the general class of potential–vorticity decompositions for the velocity field of the type

$$\mathbf{v} = \nabla\varphi + \mathbf{w}, \tag{6}$$

where $\mathbf{w}$ is any particular solution of the equation

$$\nabla \times \mathbf{w} = \zeta. \tag{7}$$

with $\zeta := \nabla \times v$ denoting the vorticity field.

The decomposition given in Eq. 6 is valid for any vector field and Eq. 7 is a necessary and sufficient condition for the validity of Eq. 6. Here, we assume $\mathbf{w}$ to be defined so as to have

$$\mathbf{w} = 0 \tag{8}$$

outside of the vortical region, V_ζ, which is defined as the region where the vorticity ζ is not negligible.

For incompressible flows, the continuity equation reads

$$\nabla \cdot \mathbf{v} = 0 \tag{9}$$

Combining with $\mathbf{v} = \nabla\varphi + \mathbf{w}$, one obtains

$$\nabla^2\varphi = \sigma, \quad \text{where} \quad \sigma = -\nabla \cdot \mathbf{w} \tag{10}$$

In order to complete the problem, the boundary conditions have to be considered. For viscous flows, the boundary condition over S_B is the no–slip condition:

$$\mathbf{v} = \mathbf{v}_B \qquad \big(\mathbf{x} \in S_B\big) \tag{11}$$

For simplicity, we introduce an additional boundary condition

$$\mathbf{w} \cdot \mathbf{n} = 0 \qquad \big(\mathbf{x} \in S_B\big) \tag{12}$$

Similarly, on the wake mid–surface S_W, we impose

$$\Delta\big(\mathbf{w} \cdot \mathbf{n}\big) = 0 \qquad \big(\mathbf{x} \in S_W\big) \tag{13}$$

Combining Eqs. 6, 11 and 12, we have, on the body surface S_B,

$$\frac{\partial\varphi}{\partial n} = \chi, \qquad \text{where} \quad \chi := \mathbf{v}_B \cdot \mathbf{n} \qquad \big(\mathbf{x} \in S_B\big) \tag{14}$$

Similarly, combining Eqs. 6 and 13, we have, on the wake mid–surface S_W,

$$\Delta\left(\frac{\partial\varphi}{\partial n}\right) = 0 \qquad \left(\mathbf{x} \in S_W\right) \tag{15}$$

In addition, in a frame of reference connected with the undisturbed air, we have

$$\varphi = O\left(\|\mathbf{x}\|^{-1}\right), \qquad \text{at infinity.} \tag{16}$$

Finally, at the trailing edge, we have (from the Joukowski smooth–flow assumption, akin to quasi–potential flows)

$$\lim_{\mathbf{x}_W \to \mathbf{x}_{TE}} \Delta\varphi(\mathbf{x}_W) = \lim_{\mathbf{x}_2 \to \mathbf{x}_{TE}} \varphi(\mathbf{x}_2) - \lim_{\mathbf{x}_1 \to \mathbf{x}_{TE}} \varphi(\mathbf{x}_1), \tag{17}$$

where 1 and 2 here denote the sides of the wing surface corresponding to the sides 1 and 2 of the wake mid–surface, respectively.

Using Eqs. 15 and 16, the boundary integral representation for the Poisson's equation, Eq. 10, is:

$$\begin{aligned} E(\mathbf{x},t)\,\varphi(\mathbf{x},t) = & \oint_{S_B}\left(\frac{\partial\varphi}{\partial n}\,G - \varphi\,\frac{\partial G}{\partial n}\right) dS(\mathbf{y}) \\ & - \int_{S_W} \Delta\varphi\,\frac{\partial G}{\partial n}\,dS(\mathbf{y}) + \int_{V_\zeta} \sigma\,G\,dV(\mathbf{y}) \end{aligned} \tag{18}$$

where $G = -1/4\pi\|\mathbf{x}-\mathbf{y}\|$. If the vortical region, V_ζ (boundary layer and wake), is sufficiently thin, we can 'compress' the volume integral into a source layer over S_B and S_W, to yield

$$\begin{aligned} E(\mathbf{x},t)\,\varphi(\mathbf{x},t) = & \oint_{S_B}\left((\chi+\chi_B)\,G - \varphi\,\frac{\partial G}{\partial n}\right) dS(\mathbf{y}) \\ & + \int_{S_W}\left(\chi_W\,G - \Delta\varphi\,\frac{\partial G}{\partial n}\right) dS(\mathbf{y}) \end{aligned} \tag{19}$$

Equation 19 is the *key* to the approach presented here since it allows one to evaluate φ anywhere in the field, if φ and $\chi+\chi_B$ over S_B, as well as $\Delta\varphi$ and χ_W over S_W are known.

The linearized Bernoulli's theorem reads:

$$p - p_\infty = -\rho\left(\dot{\varphi} + U_\infty\frac{\partial\varphi}{\partial x}\right) \tag{20}$$

The numerical formulation of the above equations can be determined both in the physical and in the Fourier domain but it is not reported here for

the sake of brevity. We just point out that, after discretization using piece–wise constant approximation and Fourier transform, the following linear relationship can be achieved:

$$\hat{p}_F = H\,\hat{p}_B. \tag{21}$$

the symbol $\hat{\cdot}$ denotes the Fourier transform of the discretized counterpart of the pressure and the equation represents the desired relationship between the field pressure (subscript F) and the boundary pressure (subscript B).

By using classical Wiener-Khintchine relationships, the above equation can be expressed in terms of the PSD matrix S_v. Thus, using Eq. 21, we have

$$S_{p_F} = H^*\,S_{p_B}\,H^T \tag{22}$$

which is the desired relationship between the PSD matrix S_{p_F} of the pressure at N_V arbitrary points in the region $\Re^3\backslash W$ and the PSD matrix S_{p_B} of the pressure at N_B points on S_B.

The expression in Eq. 22 allows one to evaluate the field–pressure PSD from the boundary–pressure PSD, thereby providing a link between two sets of experimental data (PSD of field pressure and PSD of surface pressure), often considered independent.

3 The wall pressure statistics

The random forces resulting from pressure fluctuations in the turbulent boundary layer over structural surfaces cause vibration. This surface motion becomes a source of noise which must be considered in the design of a vehicle. Therefore, the development of methods aimed at predicting interior noise levels, pressure fluctuations, and structural loading has become important in the design for instance of commercial aircraft, payload–carrying aerospace launchers, high speed trains. As pointed out by Graham (1996), in order to take into account this aspect in the design phase, there is a need for simple models capable of enhancing our physical understanding of the noise generation process and to provide relatively simple predictive formula to be utilized in the design process.

The methods of modeling and predicting sound and vibrations from a structure subject to a random pressure load, presume that the forcing function for the surface has been estimated. It can be shown [see e.g. Blake (1986) and Graham (1997)] that the excitation term is directly related to the boundary layer wavenumber-frequency spectrum that, therefore, has become the subject of many investigations. In the present discussion, we

do not enter into the details of the structural aspects, but we limit ourselves to reviewing the main features concerning the wavenumber-frequency spectrum analysis, modeling and prediction.

3.1 Relevant properties of the turbulent boundary layer

A short review of the main parameters characterizing the turbulent boundary layer and used for the scaling of the wall pressure spectra is given in the following. Extensive discussions can be found in several textbooks [see e.g. Schlichting (1979)]; therefore we limit ourselves to reviewing some relevant parameters that influence the overall statistical properties of the wall pressure fluctuations field.

At the wall, the boundary layer exerts a shear stress τ_w, and there is a strong connection between this shearing and the behavior of the flow in the immediate vicinity of the wall. As the distance from the wall increases, the influence of the wall shear on the fluid motion diminishes and the flow properties may be described in terms of the local free stream velocity U_∞ and the thickness of the boundary layer δ, this symbol denoting the so-called Blasius thickness. In this region, the flow behavior is usually called $wake-like$. Thus, depending upon the distance from the wall, two important flow regions can be identified. A layer close to the wall, where the velocity depends upon the fluid viscosity and the local wall shear, and an outer layer, where the velocity depends on the external properties of the flow (i.e. U_∞, δ and the upstream history of the layer). In the near wall region, the velocity increases linearly for increasing distance from the wall. In the outer layer the velocity defect evolves according to the well–known logarithmic law. Of course, due to the turbulent nature of the velocity field, the two regions boundaries can be defined only statistically.

In the linear region, the velocity gradient is independent of the distance from the wall. This assumption yields the following relationship:

$$U_1 = \frac{\tau_w y}{\mu} \tag{23}$$

where the subscript 1 denote the velocity component on the streamwise (x) direction and μ is the dynamic viscosity of the fluid.

In the logarithmic region the turbulence activity is the greatest and the velocity gradients are proportional to the distance from the wall. This gives rise to the logarithmic velocity profile described by the following equation:

$$\frac{U_1}{U_\tau} = \frac{1}{k} \ln\left(\frac{yU_\tau}{\nu}\right) + B \tag{24}$$

where $\ln(\cdot)$ is the natural logarithm of $\cdot$. The quantity U_τ is called the friction velocity and it is defined as

$$U_\tau = \sqrt{\frac{\tau_w}{\rho}} \tag{25}$$

being ρ the fluid density at ambient temperature. The coefficient k in Eq. 24 is the so–called Von Kàrmàn constant, equal to approximately 0.4 for any type of wall. B is a coefficient that depends only on the degree of surface roughness. The notation commonly used to represent the dimensionless quantities, is the following:

$$U^+ = \frac{U_1}{U_\tau}, \quad y^+ = \frac{yU_\tau}{\nu} \tag{26}$$

In Figure 3 a simplified scheme of the turbulent boundary layer is reported for completeness.

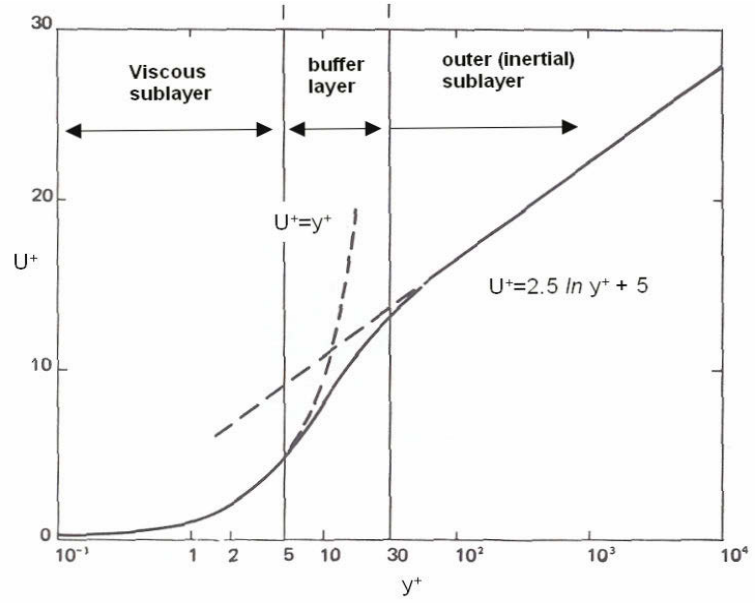

Figure 3. A scheme of the main parts of a turbulent boundary layer

Throughout the major portion of the fully developed turbulent boundary layer, the mean velocity profile over both smooth and rough walls satisfies

a defect law of the following form:

$$\frac{U_e - U_1}{U_\tau} = \frac{1}{k} \ln\left(\frac{y}{\delta}\right) + 1.38\left[2 - W\left(\frac{y}{\delta}\right)\right] \tag{27}$$

where U_e is the external velocity, outside the boundary layer. The function $W(y/\delta)$ has been introduced by Coles (1956) and it is given by:

$$W\left(\frac{y}{\delta}\right) = 1 + \sin\left[\left(\frac{y}{\delta} - \frac{1}{2}\right)\pi\right] \tag{28}$$

It is well know that the definition of the Blasius thickness δ is not suitable for turbulent boundary layers. It is better to introduce more objective definitions. Very briefly we remind the definition of displacement thickness δ^* based on a mass balance in the boundary layer and given by the following expression:

$$\delta^* = \int_0^\infty \left[\frac{U_e - U_1(y)}{U_e}\right] dy \tag{29}$$

Of course also δ^* is an *outer* scale because its magnitude is of the order of the depth of the viscous sublayer. Typically, δ^* is approximately equal to a fraction of δ, from 1/8 to 1/5, depending on the surface roughness and the pressure gradient. Similarly, another length scale can be defined on the basis of the momentum balance. It is called the momentum thickness θ and it is given by the following expression:

$$\theta = \int_0^\infty \frac{U_1(y)}{U_e}\left[\frac{U_e - U_1(y)}{U_e}\right] dy \tag{30}$$

The ratio of the two length scales is called the shape factor:

$$H = \frac{\delta^*}{\theta} \tag{31}$$

According to the laws of the wall described above, it is possible to determine explicit relationships among set of boundary layer thickness and the friction factor. We refer to more specific textbooks for the details [e.g. Schlichting (1979)].

By integrating along y, between 0 and δ, the momentum balance equation written on x, it is possible to determine an equation relating integral quantities characterizing the turbulent boundary layer. This relationship, often denoted as the Von Kàrmàn integral equation, reads:

$$\frac{C_f}{2} = \frac{d\theta}{dx} - \frac{\theta}{2}\left(\frac{2+H}{\frac{1}{2}\rho U_\infty^2}\right)\frac{dP}{dx} \tag{32}$$

C_f is the wall friction coefficient, given by:

$$C_f = \frac{\tau_w}{\frac{1}{2}\rho U_\infty^2} \tag{33}$$

Equation 32 gives the growth of the boundary layer in terms of θ as a function of the local wall shear stress coefficient and the static pressure gradient.

For a given Reynolds number $Re_x = xU_\infty/\nu$ it is possible to determine the momentum thickness by using empirical relationships. A commonly used expression, valid for smooth infinite flat plates, is the following:

$$C_f = 0.0592\ Re_x^{-\frac{1}{5}} \ \text{ for } \ Re_x \geq 10^8 \tag{34}$$

combining with Eq. 32, one obtains:

$$\frac{\theta}{x} = 0.037\ Re_x^{-\frac{1}{5}} \tag{35}$$

This equation is valid provided that

$$\frac{C_f}{\theta} \ \gg \ -(2+H)\frac{C_p}{dx} \tag{36}$$

being C_p the static pressure coefficient.

Empirical relationships are used also to determine the inner properties of the turbulent boundary layer once the outer scales are known either experimentally or numerically. In this case, by the knowledge of θ, it is possible to empirically determine C_f and then U_τ. This approach is of common use since the estimation of U_τ by the direct measurement or computation of τ_w might be very difficult in practice.

We finally remind that the velocity profile at high Reynolds numbers can be described by a power law of the following form [Schlichting (1979)]:

$$\frac{U_1}{U_\tau} = \left(\frac{y_1}{\delta}\right)^{\frac{1}{n}} \tag{37}$$

where typically $n \sim 7$ for smooth walls and 4 for rough walls. By considering the thickness definitions, the following relations are obtained:

$$\frac{\delta^*}{\delta} = \frac{1}{n+1} \tag{38}$$

and

$$\frac{\delta^*}{\theta} = \frac{n+2}{n} \tag{39}$$

For $n = 7$ it is obtained $\delta^*/\delta = 1/8$. Also Eqs. 37, 38 and 39 can be used for a qualitative estimation of the boundary layer integral properties.

3.2 Statistical properties of the wall pressure spectrum: correlations and wavenumber–frequency spectra

According to the 'weak coupling approximation' introduced above, in the present approach we consider a boundary layer developing on an infinitely extended rigid flat plate in a low Mach number flow without mean pressure gradients. In this framework, taking into account that the boundary layer thickness increases slowly in the streamwise direction, it is possible to consider the pressure field statistically homogeneous on the plane of the plate and statistically stationary in time. The homogeneous plane is described by the Cartesian axes that, for the sake of clarity, are defined as x_1, x_2, being x_1 aligned with the free stream velocity. The frame of reference adopted is depicted in Figure 4.

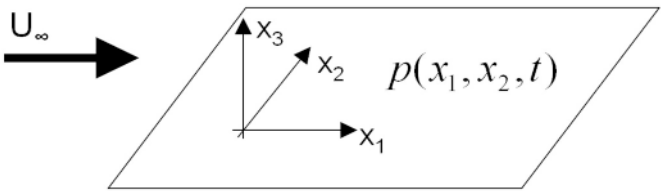

Figure 4. Frame of reference adopted to describe the statistics of pressure fluctuations.

Considering the fluctuating component of the pressure field $p(x_1, x_2, t)$, the space time correlation can be written as:

$$R_{pp}(\xi_1, \xi_2, \tau) = \frac{1}{\sigma_p^2} E[p(x_1, x_2, t)p(x_1 + \xi_1, x_2 + \xi_2, t + \tau)] \tag{40}$$

where σ_p^2 is the pressure variance and the symbol $E[\cdot]$ denotes the expected value. When the ergodic hypothesis holds, time averages can be used. This is an important hypothesis when pointwise pressure measurements are performed. In this case the pressure is a function of time only and the cross-correlation is given by a much simpler expression:

$$R_{pp}(\tau) = \frac{1}{\sigma_p^2} < p(t)p(t + \tau) >_t \tag{41}$$

where the symbol $< \cdot >_t$ now denotes the time average. Taking the Fourier transform of Eqs. 40 and 41 one obtain the wavenumber-frequency spectrum $\Phi_P(k_1, k_2, \omega)$ and the frequency spectrum $\Phi_p(\omega)$. In this notation ω is

the radian frequency and k_1, k_2 are the components of a two dimensional wavevector. By taking the frequency Fourier transform of Eq. 40 it is possible to obtain the cross-spectrum $\Gamma_p(\xi_1, \xi_2, \omega)$ that is defined in the space–frequency domain. The experimental determination not being very difficult, Γ_p represents a key ingredient for the theoretical models that are presented below.

In the framework of the statistical modeling, a relevant role is played by the phase velocity ω/k, being k the magnitude of the wavevector, whose magnitude spans from the order of the flow speed to sonic or supersonic values.

3.3 The wave–number frequency spectrum

In this section the main characteristics of the wall pressure spectrum are briefly reviewed. First, the scaling properties of the frequency spectra are discussed taking into account the most relevant experimental investigations conducted in the last 50 years. Then, illustrative examples of statistical models of the wavenumber-frequency spectrum are revised starting from the early Corcos' idea up to the most recent developments.

Scaling of the frequency spectra Due to the complex structure of the turbulent boundary layer, it is not possible to obtain a single scaling that leads to a satisfactory collapse of experimental or numerical frequency spectra $\Phi_P(\omega)$. As will be clarified below, it is possible to normalize the spectra using inner or outer variables, and a universal collapse can be obtained in various regions of the pressure spectra separately [see, among many, the early work by Willmarth (1975) and the papers by Keith, Hurdis & Abraham (1992), Farabee & Caserella (1991) and Goody *et al.* (1998)]. This is due to the fact that the wall pressure is influenced by velocity fluctuations from all parts of the boundary layer and because the convection velocity depends strongly upon the distance from the wall, as a result of the non-uniform mean velocity distribution.

For an incompressible flow, the wall pressure can be written in the form of a Poisson's equation,

$$\nabla^2 \, p(\vec{x}, t) \;=\; q(\vec{x}, t) \tag{42}$$

where $q(\vec{x}, t)$ represents the source terms. As suggested by Farabee & Caserella (1991), the analysis of the solution of the above equation in the Fourier domain, shows that the contributions to the high-frequency portion of the spectrum has mainly to be attributed to turbulence activity located in the near wall region while contributions to the lower-frequency portion

can originate from activities throughout the boundary layer. Following this physical picture, and the conjectures suggested by Bradshaw (1967) and Bull (1979), it is possible to divide $\Phi_p(\omega)$ into three main regions, depending on the frequency magnitude. At low frequencies, $\Phi_p(\omega)$ scales on outer layer variables; at high frequencies, $\Phi_p(\omega)$ is influenced by the fluid viscosity and thus it scales on inner variables; at intermediate frequencies, the shape of the spectrum is scale independent and an universal power law decay of the type ω^{-1} is expected.

Measurements of the cross-spectral densities [e.g. Bull (1967) and Farabee & Caserella (1991)] confirm that the pressure field can be divided into two distinct families, one associated with the motion in the outer layer and the other with motion in the inner layer. This separation occurs at the frequency where the auto-spectrum exhibit its maximum value. This frequency separates the non-universal from the universal scaling regimes of the frequency spectrum.

More precisely, in the low frequency region, different outer scalings have been identified. Keith, Hurdis & Abraham (1992) suggests to scale the frequency using U (the free stream velocity) and δ^*, whereas the amplitude of the pressure spectrum can be scaled through the free stream based dynamic pressure q. Other authors [including Farabee & Caserella (1991)] recommend a more effective scaling using τ_w instead of q. They suggest to scale the frequency upon U/δ and the dimensionless spectrum to be of the form $\Phi_P(\omega)U/\tau_w^2\delta$.

In the high frequency region, there is a more general consensus on the most effective scaling that is achieved through the variables U_τ, ν and τ_w. This implies that the dimensionless frequency is $\omega\nu/U_\tau^2$ and the dimensionless spectrum should be $\Phi_P(\omega)U_\tau^2/\tau_w^2$.

The universal region can be interpreted as an overlap of the two regions described above. In this part of the spectrum it is assumed $\omega\Phi_P(\omega)U/\tau_w^2 =$ constant, thus leading to the ω^{-1} scaling. A precise definition of the amplitude of the frequencies bounding the universal region can be found in Bull (1979) and Farabee & Caserella (1991).

An additional range at very low frequencies has been also identified by some authors. Farabee & Caserella (1991) determine this region at $\omega\delta^*/U \leq 0.03$ and they collapsed the spectrum using the normalization $\Phi_P(\omega)U/q^2\delta^*$. In the very low frequency region they observed the spectrum to scale as ω^2. This form of scaling is in agreement with the prediction given by the Kraichnan-Phillips theorem [Kraichnan (1956) and Phillips (1956)] which suggests that the wavenumber spectrum should scale like k^2 as $k \to 0$. According to the theoretical developments of e.g. Lilley & Hodgson (1960), this conclusion can be extended to the frequency spectrum under the hy-

pothesis of low Mach number flow conditions.

In Figure 5 a scheme summarizing the expected scalings is reported.

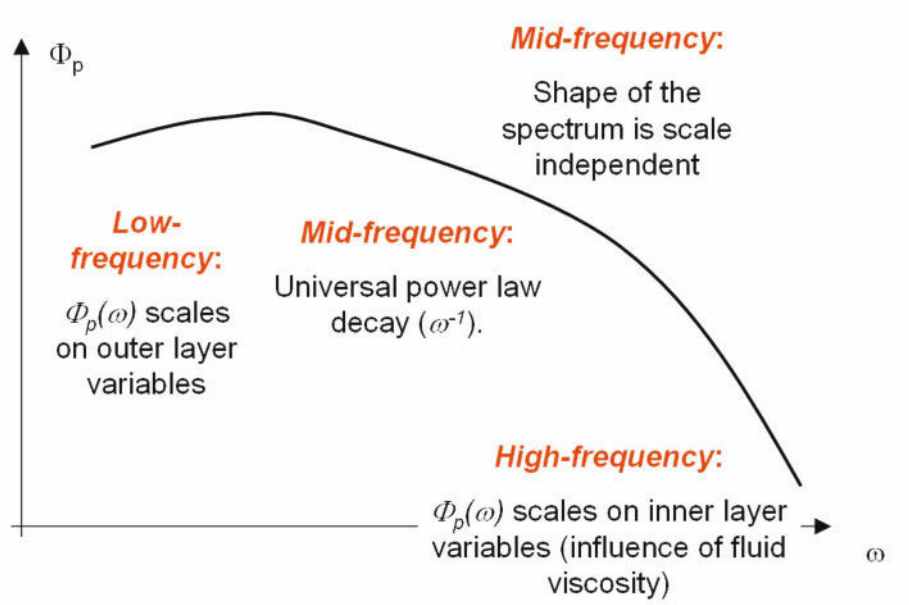

Figure 5. Sketch clarifying the expected scaling regions of a typical wall pressure auto–spectrum.

We refer to the literature [in particular Farabee & Caserella (1991) and Bull (1996)] for further discussions on the above topics and considerations about the scaling of the pressure variance.

Modeling the wavenumber-frequency spectrum According to the above discussion, several models have been proposed in the literature to reproduce the shape of the frequency auto-spectrum using suitable fits of experimental data. Here we only cite some of them as illustrative examples of common approaches. We refer to the literature for comprehensive reviews.

An early and widely used model was proposed by Corcos (1964). He gives the following representation of the frequency auto-spectrum:

$$\Phi_p(\omega) = \begin{cases} C & \text{for } \omega \leq \frac{U_e}{\delta^*} \\ C\frac{U_e}{\omega\delta^*} & \text{for } \omega > \frac{U}{\delta^*} \end{cases} \tag{43}$$

The quantity C is a dimensionless constant and U is the external velocity. Note that for $\omega > \frac{U_c}{\delta^*}$ the model correctly predicts the power law decay of the spectrum of the form ω^{-1}.

An example, among many, explaining the way the Corcos' early model has been successively modified, is given by Cousin (1999). This more general approach leads to the following expression:

$$\Phi_p(\omega) = \begin{cases} 2.14 \times 10^{-5} B & \text{for } \omega\delta^*/U_e \leq 0.25 \\ 7.56 \times 10^{-6} B \left(\omega\delta^*/U\right)^{-0.75} & \text{for } 0.25 < \omega\delta^*/U_e \leq 3.5 \\ 1.27 \times 10^{-4} B \left(\omega\delta^*/U\right)^{-3} & \text{for } \omega\delta^*/U_e > 3.5 \end{cases} \quad (44)$$

where $B = q^2\delta^*/U$.

Other formulations worth mentioning are those by Efimtsov (1986) and Chase (1987, 1991). We refer to the literature for the details.

As pointed out above, the knowledge of the frequency spectrum is not sufficient to determine the modal excitation term of a plate subject to the turbulence induced pressure filed. This quantity is directly related to the shape of the complete wavenumber-frequency spectrum of the wall pressure field. The knowledge of $\Phi_P(k_1, k_2, \omega)$ is therefore fundamental to compute the response of a surface panel subject to the action of the random pressure load.

As pointed out by Bull (1996), the highest spectral levels of the pressure fluctuations are associated to the mean flow convection and, in the wavenumber spectrum, are centered on a wavenumber $k_1 = \omega/U_c$, k_1 along the free stream velocity. This part of the spectrum is often referred to as the convective ridge. For $k_1 \ll \omega/U_c$ the spectrum is expected to be independent of the wavenumber. Another important aspect is related to the so-called sonic wavenumber $k_0 = \omega/c$. According to Blake (1986), for $k = k_0$ an apparent singularity is present in the spectrum. However, in real flows, the wavenumber-frequency spectrum is expected to have a local finite peak in the vicinity of k_0. These are among the main features that an analytical model attempting to predict the $\Phi_p(k_1, k_2, \omega)$ shape, have to reproduce correctly.

One of the most reliable model developed in literature is again the early approach proposed by Corcos (1964) and based on the Fourier transform of a curve fit of measured narrow band pressure correlations. According to extensive experimental measurements [namely Willmarth (1975) and Bull (1967)], the cross-spectral density $\Gamma_p(\xi_1, \xi_2, \omega)$ can be represented as:

$$\Gamma_p(\xi_1, \xi_2, \omega) = \Phi_p(\omega)\, A(\omega\xi_1/U_c)\, B(\omega\xi_2/U_c)\, e^{i\omega\xi_1/U_c} \quad (45)$$

where

$$A(\omega\xi_1/U_c) = e^{-\alpha_1|\omega\xi_1|/U_c} \text{ and } B(\omega\xi_2/U_c) = e^{-\alpha_2|\omega\xi_2|/U_c}$$

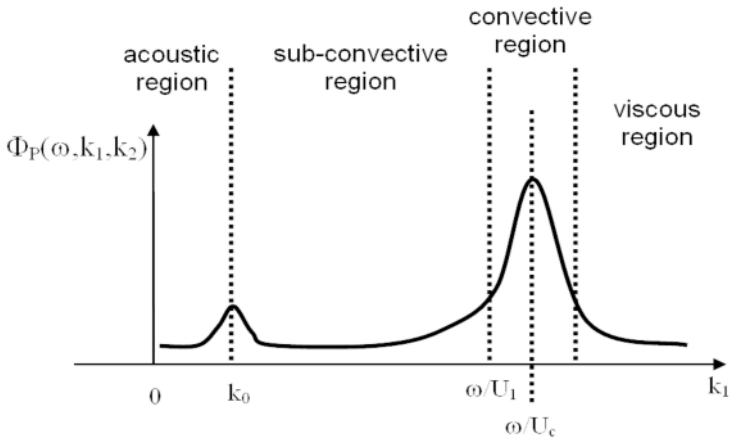

Figure 6. A scheme representing the wavenumber-frequency spectrum as a function of wavenumber, at constant frequency (scheme adapted from Blake (1986)).

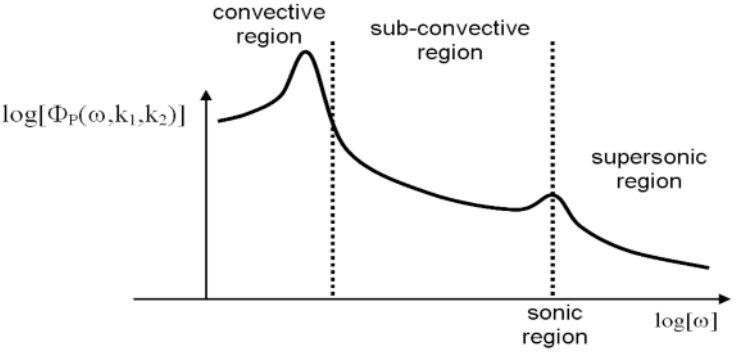

Figure 7. A scheme representing the wavenumber-frequency spectrum as a function of frequency, at constant wavenumber (scheme adapted from Blake (1986)).

whereas U_c is the convection velocity and α_1 and α_2 are parameters chosen to yield the best agreement with experiments. Various values are given in the literature. The typical range of the values is $\alpha_1 = 0.11 \div 0.12$ and $\alpha_2 = 0.7 \div 1.2$ for smooth rigid walls.

Unfortunately, only few experimental or numerical data concerning direct measurements of the wavenumber–frequency spectrum are available in the literature [Abraham (1998), Choi & Moin (1990), Panton & Robert (1994), Farabee & Geib (1991), Hwang & Maidanik (1990), Manoha (1996)]. However, it appears evident that a big spread is present in the low wavenumber range and that the Corcos model overpredicts levels at wavenumbers below the convective peak. This point is crucial for many applications, in particular in the case of underwater and surface marine vehicles and for aeronautical structures above the aerodynamic coincidence frequency [see also Ciappi *et al.* (2009)]. Later workers used analytical or quasi analytical approaches, or revised versions of the Corcos approach, in attempts to describe this region more accurately [see e.g. Graham (1997) for details].

Most of the models proposed continued to follow the philosophy of the Corcos approach that can be generalized as follows. A first common feature of those empirical models is the separation of variables approach to represent the correlation function dependence on the streamwise separation ξ_1 and the crossflow separation ξ_2. This is known as the 'multiplication hypothesis' in which the coherence of the cross-spectral density for an arbitrary separation direction is formed by the product of the cross-spectral densities for streamwise and spanwise separations, respectively. The axisymmetry of the geometry and of the flow is usually not explicit in those formulations but it is accounted for through the adjustable coefficients. According to the Corcos idea given in Eq. 45, most of the models suggest to take exponential decaying form of the functions A and B,

$$A(\omega, \xi_1) = e^{-\frac{|\xi_1|}{L_1(\omega)}} \text{ and } B(\omega, \xi_2) = e^{-\frac{|\xi_2|}{L_2(\omega)}} \tag{46}$$

where L_1 and L_2 are the so-called coherence lengths in the streamwise and spanwise direction respectively.

The main advantage of adopting the expression given in Eqs. 45 and 46 is that the auto-spectrum part is decoupled from the cross-spectrum part. That implies that any choice for modeling the function $\Phi_p(\omega)$, as those described above, can be addressed independently of any choice for representing the functions L_1 and L_2.

As for auto-spectra, Cousin modified the Corcos model yielding the fol-

lowing expressions of the coherence lengths:

$$\begin{aligned} L_1 &= \frac{U_c}{\omega\alpha_1}\left\{1+\left(\frac{U_c}{\omega b_M \delta}\right)^2\right\}^{-1/2} \\ L_2 &= \frac{U_c}{\omega\alpha_2}\left\{1+\left(\frac{U_c}{\omega b_T \delta}\right)^2\right\}^{-1/2} \end{aligned} \tag{47}$$

where $U_c = 0.75U$, $b_M = 0.756$, $b_T = 0.378$. $\alpha_1 = 0.115$ for smooth walls and 0.32 for rough walls, whereas $\alpha_2 = 0.32$ in all cases.

A similar model, not reported here for brevity, has been proposed by Cockburn & Robertson (1974). Wu & Maestrello (1995) proposed a model where the flow is assumed semi-frozen and decaying in space and time at a constant velocity U_c. After performing a comprehensive set of experimental results of wind tunnel testing, they defined an ensemble average of the cross correlation for the pressure fluctuation due to the turbulent boundary layer in which the effects of the Reynolds number and the boundary layer thickness were included.

Other models proposed by Chase (1980), Efimtsov (1982), Ffowcs Williams (1982), Chase (1987) and Smol'yakov & Tkachenko (1991) are compared in Graham (1997) and a plot reporting the spectra predicted by different models is given in Figure 8. It is shown that even at the convective peak, a relevant scattering among the model predictions is evident. Even larger scattering is observed in the estimation of the radiated sound as reported in the same paper.

The best model for high speed aircraft is, according to Graham, the one which provides an accurate description of the convective peak. Efimtsov's model, an extension of Corcos model, is cited as a suitable candidate. For the sake of completeness, we report in the following the Efimtsov idea:

$$\begin{aligned} L_1 &= \delta\left[\left(\frac{a_1 St_\tau}{U_c/U_\tau}\right)^2 + \frac{a_2^2}{St_\tau^2+(a_2/a_3)^2}\right]^{-1/2} && \text{for} \quad 0.41 < M < 2.1 \\ L_2 &= \delta\left[\left(\frac{a_4 St_\tau}{U_c/U_\tau}\right)^2 + \frac{a_5^2}{St_\tau^2+(a_5/a_6)^2}\right]^{-1/2} && \text{for} \quad M < 0.75 \\ L_2 &= \delta\left[\left(\frac{a_4 St_\tau}{U_c/U_\tau}\right)^2 + a_7^2\right]^{-1/2} && \text{for} \quad M > 0.9 \end{aligned} \tag{48}$$

In this model $U_c = 0.75U_e$ and $St_\tau = \omega\delta/U_\tau$ is a Strouhal number defined on the friction velocity. Averaged values of the empirical constants are $a_1 = 0.1$, $a_2 = 72.8$, $a_3 = 1.54$, $a_4 = 0.77$, $a_5 = 548$, $a_6 = 13.5$, $a_7 = 5.66$. It can be shown that at high frequencies, these expressions correspond to a Corcos model with $\alpha_1 = 0.1$ and $\alpha_2 = 0.7$. Even though the number of

empirical constants is relevant, the model is extensively used thanks to the introduction of the Mach number as a relevant parameter.

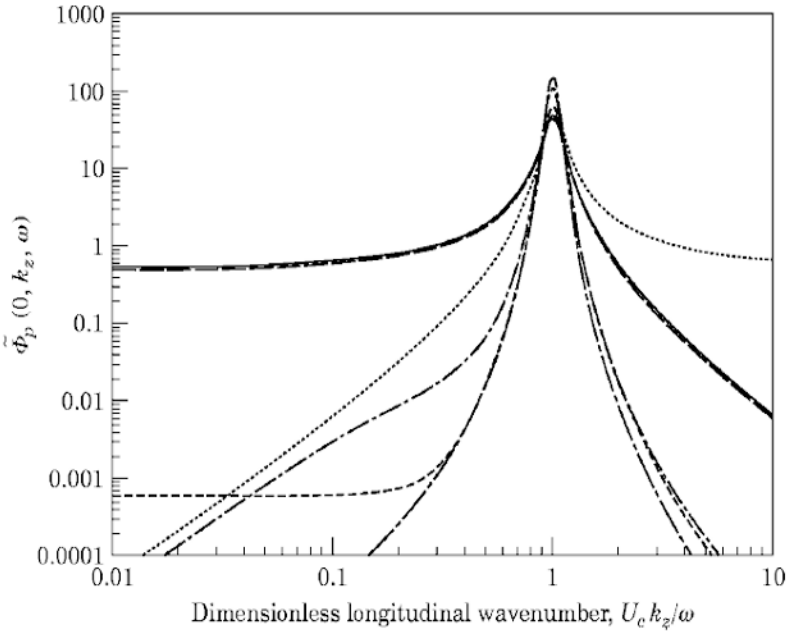

Figure 8. Wavenumber frequency spectra computed at a fixed frequency as reported in Graham (1997). The spectra are computed as functions of the longitudinal wavenumber non-dimensionalized on the convective wavenumber ω/U_C (courtesy of JSV).

More recently, Singer (1996a) and Singer (1996b) performed a Large-Eddy Simulation (LES) of a turbulent boundary layer at relatively high Reynolds number and proposed a model that overcomes the 'multiplication hypothesis' that is the basis of all the models based on the Corcos' philosophy. His approach is based on an accurate fit of the two-dimensional coherence and therefore is particularly efficient for the determination of the off-axis coherences.

To the best of our knowledge, the most recent model proposed in literature is the one presented by Finneveden *et al.* (2005). They suggested a modified version of the Corcos and of the Chase model, thus going back to the 'multiplication hypothesis'. They demonstrated that it is possible

to find for both models a complete set of free parameters that provide a fair agreement with experimental data. The key point was to modify the Corcos model by introducing a frequency and flow speed dependence in the parameters and to introduce two new parameters in the Chase model to better fit the spanwise coherence to measurements.

3.4 Coherent structures and wall pressure fluctuations

As pointed out above, it is possible to establish a connection between the wall pressure wavenumber spectra and physical quantities describing the turbulent boundary layer. In particular, the high wavenumber components should be attributed to fluid dynamic structures in the near wall region while the low wavenumber domain is influenced by the large scale structures in the outer layer. However, the detailed features of organized events that occur in the boundary layer are lost by the unconditional averaging techniques used in obtaining spectral estimates of the pressure field. This is an important issue from the practical viewpoint since a deeper knowledge of the fluid dynamic structures underlying the observed pressure properties may be helpful to address suitable control strategies aimed at manipulating the flow structures and modifying the wall pressure behavior.

Numerical simulations of simplified configurations attempted to clarify the connection between wall pressure fields and near wall vortical structures whose topology was selected a-priori according to classical conceptual models of the turbulent boundary layer. For example, Dhanak & Dowling (1995) and Dhanak, Dowling & Si (1997), following the conceptual model of the boundary layer proposed by Orlandi & Jimenez (1994), were able to clarify the effect of near wall quasi-streamwise structures upon the wall pressure field. More recently, Ahn, Graham & Rizzi (2004) and Ahn, Graham & Rizzi (2010) reproduced correlations and spectra at the wall. In order to estimate the wall pressure distribution, they reproduced hairpin vortex dynamics on the basis of the so called attached eddy model proposed by Perry & Chong (1982).

Only a few experiments have been focused on these aspects, since the correlation between wall pressure and coherent structures is rather difficult to interpret due to the chaotic nature of the pressure field. Among the existing studies, the work by Johansson, Her & Haritonidis (1987) can be mentioned: they carried out simultaneous pressure–velocity measurements and suggested physical mechanisms for the underlying generation of positive or negative pressure peaks at the wall. However, they did not clarify the connection between the educed structures and the wall pressure spectral quantities.

In a recent paper, Camussi, Robert & Jacob (2008) applied non conventional time-frequency post-processing tools to analyze wall pressure experimental data. The application of multi-variate wavelet transform permitted them to establish a connection between sweep/ejections events and large pressure coherence. More specifically, using a conditional sampling technique, they observed that averaged pressure signatures due to hydrodynamic effects were composed of a large negative pressure drop coupled to a weaker positive bump. This behavior was ascribed to accelerated-decelerated motions within the turbulent boundary layer.

The presence of a positive pressure bump coupled with a stronger negative pressure drop was also observed by Dhanak & Dowling (1995) who simulated numerically the pressure field induced at the wall by streamwise vortices. Similarly, in an experiment performed by Johansson, Her & Haritonidis (1987) negative–positive pressure jumps were also observed and were identified as $burst-sweep$ events. The conditional results of Johansson, Her & Haritonidis (1987) were obtained by correlating pressure negative peaks with velocity events found in the buffer region of the boundary layer through the so–called VITA technique [see e.g. Blackwelder & Kaplan (1976)].

Analogous conclusions were driven by Jayasundera, Casarella & Russell (1996) through the investigation of experimental wall pressure and inflow velocity data and the application of coherent structures identification techniques. They showed that the organized structures present within the turbulent boundary layer contain both ejection and sweep motions inducing positive and negative pressure events respectively.

More recently, Kim, Choi & Sung (2002) attempted to correlate the wall pressure fluctuations with the streamwise vortices of a numerically simulated turbulent boundary layer. They suggest that the high negative wall pressure fluctuations are due to outward motion in the vicinity of the wall correlated to the presence of streamwise vortices.

3.5 Effect of adverse pressure gradient and separation

An overall effect of adverse pressure gradients onto the wall pressure field statistics is an increase of the wall pressure fluctuations and a reduction of the convection velocity. This behavior was first observed by Schloemer (1967) through an experimental study devoted to the investigation of the influence of a mild adverse pressure gradient on wall pressure fluctuations. Owing to changes in the streamwise turbulent intensity, Schloemer also noticed an increase in the wall pressure spectral densities at low-frequencies (in outer scaling), whereas little effect was observed in the high-frequency range. This result has been later confirmed [see e.g. Lim (1971)] and seems

to suggest that the pressure gradient influences the outer layer region which, as described above, is directly correlated to the mid and low frequency range of the wall pressure frequency spectra.

Na & Moin (1998) performed a Direct Numerical Simulation (DNS) of a turbulent boundary layer developing over a flat plate, under both mild and strong imposed adverse pressure gradient. In the latter case (involving extensive separation) the frequency spectra in the separation bubble were found to exhibit a ω^{-4} decay, whereas a ω^{-2} behavior at high frequencies was observed for the spectra downstream of the reattachment position. The analysis of two-point correlations of wall pressure fluctuations also revealed strong coherence in the spanwise direction, that was attributed to the occurrence of large two-dimensional roller-type vortical structures. These authors also showed that the presence of flow separations, re-circulations and re-attachments lead to the generation of wall pressure fluctuations whose overall level might be significantly larger (up to 30dB) than that observed in equilibrium turbulent boundary layer with no separations.

Measurements of surface pressure fluctuations for a separated turbulent boundary layer under adverse pressure gradient were reported by Simpson, Ghodbane & McGrath (1987). Those authors found that pressure fluctuations increase monotonically through the adverse pressure gradient region, and showed that the maximum turbulent shear stress in the wall-normal direction can be used as a scaling variable since it yields good collapse of the normalized spectra at various streamwise stations.

Several studies have been conducted to characterize the fluid dynamic structure of flows whose separation is induced by a surface discontinuity. Detailed results have been obtained for several geometries, including backward facing steps [see Simpson (1989), and the literature cited therein for a comprehensive review in the field], sharp edges [as in Kiya, Sasaki & Arie (1982), Kiya & Sasaki (1985), and Hudy, Naguib & Humphreys (2003)], inclined surfaces [e.g. Song, DeGraaff & Eaton (2000)] and surface bumps [e.g. Kim & Sung (2006)]. Most of these studies have shown that the wall pressure fluctuations are driven by a low frequency excitation linked to the expansion and contraction of the separation bubble, a phenomenon usually designated as flapping motion. Besides, the vortical structures within the shear layer have been identified as the source of higher frequency peaks normally observed close to the reattachment position.

Stüer, Gyr & Kinzelbach (1999) analyzed the separation bubble upstream of a Forward Facing Step (FFS) in laminar flow conditions through flow visualizations and particle tracking velocimetry measurements. They demonstrated that the laminar re-circulating region upstream of the step is an open separation bubble characterized by spanwise quasi-periodic un-

steadiness. The flow topology and the pressure field upstream and downstream of an FFS at much higher Reynolds numbers have been recently studied by Largeau & Moriniere (2007). The effect of the relevant length-scales has been underlined in this work and the influence of the flapping motion upon the pressure field at the reattachment point has been demonstrated by means of pressure-velocity cross-correlations obtained from simultaneous wall microphones and hot wire anemometry measurements. Fourier pressure spectra upstream and downstream of a FFS have been presented also by Efimtzov *et al.* (1999) who showed that the region downstream of the step is the most significant in terms of pressure level. On the other hand, Leclercq *et al.* (2001) considered the acoustic field induced by a forward-backward step sequence and suggested that the most effective region in terms of noise emission is located just upstream of the FFS. The experimental results reported in Leclercq *et al.* (2001) have been successfully reproduced in a large eddy simulation performed by the same group, Addad *et al.* (2003). It was confirmed that the largest acoustic source is located in the separated region upstream of the wall discontinuity. Camussi, Guj & Ragni (2006) and Camussi *et al.* (2006) measured the pressure fluctuations at the wall of a shallow cavity representing a backward-forward step sequence. The authors again showed that the region close to the FFS is the most effective in terms of wall pressure fluctuations level even though the origin of the observed acoustic field was not clarified. In a recent study of the incompressible flow past a forward-facing step, Camussi *et al.* (2008) also observed the increase of energy at low-frequencies and a decrease at higher ones.

A flow separation can be induced also by the effect of a shockwave interacting with the boundary layer, a situation that can typically be encountered in transonic flow conditions. The prediction of pressure fluctuations in the transonic regime is particularly important in the vibro-acoustic design of aerospace launch vehicles. As a matter of fact, vibrations induced in the interior of the vehicle can exceed design specifications, and cause payload damage, as well as structural damage due to fatigue problems.

The presence of a shockwave and the consequent separation, causes an adverse pressure gradient that modifies significantly the boundary layer dynamics and causes substantial modification of the wall pressure signature. The Mach number effect in attached boundary layers has been taken into account in a few literature models [see e.g. the one proposed by Efimtsov (1982) and cited above]. On the other hand, the effect of the shockwave induced separation on the wavenumber-frequency spectrum is the subject of quite a few literature papers. We remind the numerical studies conducted by Pirozzoli and co-workers [Pirozzoli, Bernardini & Grasso (2010)

and Bernardini, Pirozzoli & Grasso (2011)] based on a DNS approach used to simulate the shockwave induced separation on a flat plate at a transonic Mach number ($M = 1.3$). They show that the shape of the frequency wall pressure spectra is qualitatively modified by the interaction with the shock wave. In the region with zero pressure gradient, the shape of the spectra is similar to that observed in low-speed boundary layers. When the pressure gradient is relevant, the low-frequency components of the spectrum are enhanced while the higher ones are attenuated. This observation is in agreement with results obtained in low-speed boundary layers in adverse pressure gradient and it is the signature of the greater importance of large-scale, low-frequency dynamics past the interacting shock, with respect to the fine scale effects. According to observations in low speed flows upstream an FFS by Camussi *et al.* (2008), in the separated region downstream of the shock, a self-similar structure of the pressure spectra is observed exhibiting the -7/3 inertial scaling at intermediate frequencies and a -5 decay law at high frequencies.

Similar scalings were observed in transonic and supersonic flow conditions by Camussi *et al.* (2007). They analyzed the statistics of the wall pressure fluctuations on a scaled model of an aerospace launcher that has been investigated in transonic and supersonic wind tunnels. Even though qualitatively, the -1 and -7/3 scalings were documented at several stations along the surface of the model.

The determination of a general predictive model for the wavenumber–frequency spectrum in the presence of shockwaves is however still far and, to the authors' opinion, this topic merits to be the task for future extensive research.

3.6 Concluding remarks

A brief overview of the studies made in the field of boundary layer noise in the last 60 years, has been reported, with particular emphasis on the interior noise problem and the mechanisms underlying the generation of the wall pressure fluctuations responsible for the panel vibrations and the transmission of noise.

The problem of the acoustic radiation due to the interaction of a turbulent boundary layer with a solid surface, has been treated only qualitatively. The prediction of the far field noise can be achieved by integral formulations and the main feature outlined in the present notes consisted in an order of magnitude estimation of the terms representing the far field pressure solution. The practical consequences of those results have been discussed in the framework of the airframe noise problem.

More emphasis has been given on the description of the wall pressure statistics mainly in terms of their spectral content estimated in the Fourier domain. The scaling parameters of the frequency spectra have been discussed in connection with the properties of the near wall and the outer–layer regions of the turbulent boundary layer. The main properties of the wavenumber-frequency spectra have been also reviewed and discussed along with the main statistical models proposed in literature to predict the auto– and cross–spectra behaviors.

More practical aspects have been treated by considering the case of separated flows and the complex behavior arising by the interaction of the boundary layer with shockwaves.

Bibliography

B.M. Abraham, *Direct measurements of the turbulent boundary layer wall pressure wavenumber–frequency spectra*, Journal of Fluids Engineering 120, pages 29–39, 1998.

Y. Addad, D. Laurence, C. Talotte and M.C. Jacob, *Large eddy simulation of a forward-backward facing step for acoustic source identification*, International Journal of Heat and Fluid Flow 24, pages 562–571, 2003.

B-K. Ahn, W.R. Graham and S.A. Rizzi, *Modelling unsteady wall pressures beneath turbolent boundary layers*, 10th CEAS/AIAA Aeroacoustics Conference, 10-12 May 2004, Manchester, UK, 2004.

B-K. Ahn, W.R. Graham and S.A. Rizzi, *A structure-based model for turbulent-boundary-layer wall pressures*, Journal of Fluid Mechanics 650, pages 443–478, 2010.

R.F. Blackwelder and R.E. Kaplan, *On the wall structure of the turbulent boundary layer*, Journal of Fluid Mechanics 76, pages 89–112, 1976.

W.K. Blake, Mechanics of flow-induced sound and vibration. Volume II: Complex flow-structure interactions, Academic Press, 1986.

P. Bradshaw, *'Inactive' motion and pressure fluctuations in turbulent boundary layers*, Journal of Fluid Mechanics 30, pages 241-258, 1967.

M.K. Bull, *Wall pressure fluctuations associated with subsonic turbulent boundary layer flow*, Journal of Fluid Mechanics 28, pages 719–754, 1967.

M.K. Bull, *On the form of the wall-pressure spectrum in a turbulent boundary layer in relation to noise generation by boundary layer-surface interactions*, Mechanics of Sound Generation in Flows, IUTAM Conference, Springer-Verlag, Berlin, pages 210–216, 1979.

M.K. Bull, *Wall-pressure fluctuations beneath turbulent boundary layers: some reflections of forty years of research*, Journal of Sound and Vibration 190(3), pages 299–315, 1996.

R. Camussi, G. Guj and A. Ragni, *Wall pressure fluctuations induced by turbulent boundary layers over surface discontinuities*, Journal of Sound and Vibration 294, pages 177–204, 2006.

R. Camussi, G. Guj, A. Di Marco and A. Ragni, *Propagation of wall pressure perturbations in a large aspect-ratio shallow cavity*, Experiments in Fluids 40, pages 612–621, 2006.

R. Camussi, G. Guj, B. Imperatore, A. Pizzicaroli and D. Perigo, *Wall pressure fluctuations induced by transonic boundary layers on a launcher model*, Aerospace Science and Technology 11, pages 349–359, 2007.

R. Camussi, G. Robert and M.C. Jacob, *Cross–wavelet analysis of wall pressure fluctuations beneath incompressible turbulent boundary layers*, Journal of Fluid Mechanics 617, pages 11–30, 2008.

R. Camussi, M. Felli, F. Pereira, G. Aloisio and A. Di Marco, *Statistical properties of wall pressure fluctuations over a forward-facing step*, Physics of Fluids 20, pages 075113-1 – 075113-13, 2008.

D. Chase, *Modelling the wavevector-frequency spectrum of turbulent boundary layer wall pressure*, Journal of Sound and Vibration 70, pages 29–67, 1980.

D.M. Chase, *The character of the turbulent wall pressure spectrum at subconvective wavenumbers and a suggested comprehensive model*, Journal of Sound and Vibration 112, pages 125–147, 1987.

D.M. Chase, *Fluctuations in wall-shear stress and pressure at low streamwise wavenumbers in turbulent boundary-layer flow*, Journal of Fluid Mechanics 225, pages 545–556, 1991.

H. Choi and P. Moin *On the space–time characteristics of wall pressure fluctuations*, Physics of Fluids A 2, pages 1450–1460, 1990.

E. Ciappi, F. Mangionesi, S. De Rosa and F. Franco, *Hydrodynamic and hydroelastic analyses of a plate excited by the turbulent boundary layer*, Journal of Fluids and Structures 258, pages 321–342, 2009.

J.A. Cockburn and J.E. Robertson, *Vibration response of spacecraft shrouds to in-flight fluctuating pressures*, Journal of Sound and Vibration 33, pages 399–425, 1974.

D. Coles, *The law of the wake in the turbulent boundary layer*, Journal of Fluid Mechanics 1, pages 191-226, 1956.

G.M. Corcos, *The structure of the turbulent pressure field in boundary-layer flows*, Journal of Fluid Mechanics 18(3), pages 353–378, 1964.

G. Cousin, *Sound from TBL induced vibrations*, PhD Thesis, KTH Marcus Wallenberg Laboratory for Sound and Vibration Research, Stockholm, 1999.

N. Curle, *The influence of solid boundaries upon aerodynamic sound*, Proceedings of the Royal Society of London A231, pages 505–514, 1955.

M.R. Dhanak and A.P. Dowling, *On the pressure fluctuations induced by coherent cortex motion near a surface*, Proc. 26th AIAA Fluid Dynamics Conference, June 1995, Paper No. 95-2240, 1995.

M.R. Dhanak, A.P. Dowling and C. Si, *Coherent vortex model for surface pressure fluctuations induced by the wall region of a turbulent boundary layer*, Physics of Fluids A 9, pages 2716–2731, 1997.

A.P. Dowling, *Flow-acoustic interaction near a flexible wall*, Journal of Fluid Mechanics 128, pages 181–198, 1983.

B.M. Efimtsov, *Characteristics of the field of turbulent wall pressure fluctuations at large Reynolds numbers*, Soviet Physics - Acoustics 28, pages 289–292, 1982.

B.M. Efimtsov, *Vibrations of a cylindrical panel in a field of turbulent pressure fluctuations*, Soviet Physics - Acoustics 32(4), pages 336–337, 1986.

M. Efimtsov, N.M. Kozlov, S.V. Kravchenko and A.O. Anderson, *Wall pressure fluctuation spectra at small forward-facing step*, Proceedings of the Fifth AIAA/CEAS Aeroacoustics Conference, Bellevue WA, AIAA Paper No. 99-1964, 1999.

T. M. Farabee and M. J. Casarella, *Spectral features of wall pressure fluctuations beneath turbulent boundary layers*, Physics of Fluids A 3(10), pages 2410–2420, 1991.

T.M. Farabee and F.E. Geib, *Measurements of boundary layer pressure fluctuations at low wavenumbers on smooth and rough walls*, ASME Symposium on Flow Noise Modelling, Measurement and Control, NCA-vol. 11, FED-vol. 130, pages 55–68, 1991.

J.E. Ffowcs Williams, *Boundary-layer pressures and the Corcos model: a development to incorporate low wavenumber constraints*, Journal of Fluid Mechanics 125, pages 9–25, 1982.

J.E. Ffowcs Williams and D.L. Hawkings, *Sound Generated by Turbulence and Surfaces in Arbitrary Motion*, Philosophical Transactions of the Royal Society A264, pages 321–342, 1969.

S. Finnveden, F. Birgersson, U. Ross and T. Kremer, *A model of wall pressure correlation for prediction of turbulence–induced vibration*, Journal of Fluids and Structures 20, pages 1127-1143, 2005.

M.C. Goody, R.L. Simpson, M. Engel, C.J. Chesnakas and W.J. Devenport, *Mean velocity and pressure and velocity spectral measurements within a separated flow around a prolate spheroid at incidence*, AIAA Paper 98-0630, 1998.

W.R. Graham, *Boundary layer induced noise in aircraft. Part I: The flat plate model*, Journal of Sound and Vibration 192, pages 101–120, 1996.

W.R. Graham, *A comparison of models for the wavenumber-frequency spectrum of turbolent boundary layer pressures*, Journal of Sound and Vibration 206(4), pages 541–565, 1997.

M.S. Howe, *The wall-pressure spectrum in turbulent flow over a randomly inhomogeneous elastic solid*, Journal of the Acoustical Society of America 91(1), pages 91–98, 1992.

M.S. Howe, Acoustics of Fluid: Structure Interactions, Cambridge University Press, London, 1998.

Z. Hu, C.L. Morfey and N.D. Sandham, *Aeroacoustics of wall-bounded turbulent flows*, AIAA Journal 40, pages 465–473, 2002.

Z. Hu, C.L. Morfey and N.D. Sandham, *Sound radiation in turbulent channel flows*, Journal of Fluid Mechanics 475, pages 269–302, 2003.

H. Hubbard, *Aerodynamic noise and the plane boundary*, Aeroacoustics of flight vehicles: theory and practice, volume 1: noise sources (D. Crighton: 'Airframe noise', pp. 391-447), NASA RP-1258, 1991.

M. Hudy, A.M. Naguib and W.M. Humphreys Jr., *Wall-pressure array measurements beneath a separating/reattaching flow region*, Physics of Fluids 15, pages 706–717, 2003.

Y.F. Hwang and G. Maidanik, *A wavenumber analysis of the coupling of a structural mode and flow turbulence*, Journal of Sound and Vibration 142, pages 135–152, 1990.

S. Jayasundera, M.J. Casarella and S.J. Russell, *Identification of coherent motions using wall-pressure signatures*, Tech. Rep. 19960918-036, Catholic Univ. of America, Washington DC, 1996.

A.V. Johansson, J.-Y. Her and J.H. Haritonidis, *On the generation of high-amplitude wall-pressure peaks in turbulent boundary layers and spots*, Journal of Fluid Mechanics 175, pages 119–142, 1987.

W.L. Keith, D.A. Hurdis and B.M. Abraham, *A comparison of turbulent boundary layer wall-pressure spectra*, Journal of Fluids Engineering 114, pages 338–347, 1992.

J. Kim, J.-I. Choi and H.J. Sung, *Relationship between wall pressure fluctuations and streamwise vortices in a turbulent boundary layer*, Physics of Fluids 14, pages 898–901, 2002.

J. Kim and H.J. Sung, *Wall pressure fluctuations and flow induced noise in a turbulent boundary layer over a bump*, Journal of Fluid Mechanics 558, pages 79–102, 2006.

A. Kiya, K. Sasaki and M. Arie, *Discrete-vortex simulation of a turbulent separation bubble*, Journal of Fluid Mechanics 120, pages 219–244, 1983.

A. Kiya and K. Sasaki, *Structure of large-scale vortices and unsteady reverse flow in the reattaching zone of a turbulent separation bubble*, Journal of Fluid Mechanics 154, pages 463–491, 1985.

R.H. Kraichnan, *Pressure fluctuations in turbulent flow over a flat plate*, The Journal of the Acoustical Society of America 28, pages 278–390, 1956.

J. Largeau and V. Moriniere, *Wall pressure fluctuations and topology in separated flows over a forward-facing step*, Experiments in Fluids 42(1), pages 21–40, 2007.

D.J.J. Leclercq, M.C. Jacob, A. Louisot and C. Talotte, *Forward–backward facing step pair: Aerodynamic flow, wall pressure and acoustic characterization*, Proceedings of the Seventh AIAA/CEAS Aeroacoustics Conference, Maastricht, The Netherland, AIAA Paper No. 2001-1249, 2001.

M.J. Lighthill, *On sound generated aerodinamically. Part I: General Theory*, Proceedings of the Royal Society of London A211, pages 564–587, 1952.

G.M. Lilley and T.H. Hodgson, *On surface pressure fluctuations in turbulent boundary layers*, AGARD Report No. 276, 1960.

K.B. Lim, *A study of pressure fluctuations in turbulent shear flows under the effects of mean pressure gradients*, PhD thesis, Department of Mechanical Engineering, University of Adelaide, 1971.

E. Manoha, *The wavenumber-frequency spectrum of the wall pressure fluctuations beneath a turbulent boundary layer*, Proceedings of AIAA/CEAS Aeroacoustics Conf., May 6-8, State College, PA, AIAA paper 96-1758, 1996.

L. Morino, C. Leotardi and R. Camussi, *Power spectral density transfer function from boundary-pressure to field-pressure*, Proc. 16th AIAA/CEAS Aeroacoustics Conference, Stockholm (Swe), AIAA paper 2010–3993, 2010.

Y. Na and P. Moin, *The structure of wall-pressure fluctuations in turbulent boundary layers with adverse pressure gradient and separation*, Journal of Fluid Mechanics 377, pages 347–373, 1998.

P. Orlandi and J. Jimenez, *On the generation of turbulent wall friction*, Physics of Fluids 6, pages 634–641, 1994.

R.L. Panton and G. Robert, *The wavenumber-phase velocity representation for the turbulent wall-pressure spectrum*, Journal of Fluid Engineering 116, page 447, 1994.

A.E. Perry and M.S. Chong, *On the mechanism of wall turbulence*, Journal of Fluid Mechanics 119, pages 173–217, 1982.

O.M. Phillips, *On the aerodynamic surface sound from a plane turbulent boundary layer*, Proceedings of the Royal Society of London, Series A, Vol. 234, pages 327–335, 1956.

S. Pirozzoli, M. Bernardini and F. Grasso, *Direct numerical simulation of transonic shock/boundary layer interaction under conditions of incipient separation*, Journal of Fluid Mechanics 657, pages 361–393, 2010.

M. Bernardini, S. Pirozzoli and F. Grasso, *The wall pressure signature of transonic shock/boundary layer interaction*, Journal of Fluid Mechanics 671, pages 288–312, 2011.

A. Powell, *The influence of solid boundaries upon aerodynamic sound*, Proceedings of the Royal Society of London A231, pages 962–990, 1960.

A. Powell, *Aerodynamic noise and the plane boundary*, Journal of the Acoustical Society of America 32, pages 982–990, 1960.

H. Schlichting, Boundary-Layer Theory, McGraw-Hill, New York, 1979.

H.H. Schloemer, *Effects of pressure gradient on turbulent-boundary-layer wall-pressure fluctuations*, Journal of the Acoustical Society of America 42(1), pages 93–113, 1967.

K. Shariff and M. Wang, *A numerical experiment to determine whether surface shear-stress fluctuations are a true sound source*, Physics of Fluids 17, pages 107105-1–107105-11, 2005.

R.L. Simpson, M. Ghodbane and B.E. McGrath, *Surface pressure fluctuations in a separating turbulent boundary layer*, Journal of Fluid Mechanics 177, pages 167–186, 1987.

R.L. Simpson *Turbulent boundary-layer separation*, Annual Review of Fluid Mechanics 21, pages 205–234, 1989.

B.A. Singer, *Turbulent wall-pressure fluctuations: new model for off-axis cross-spectral density*, NASA Contractor Report 198297, 1996.

B.A. Singer, *Large-eddy simulation of turbulent wall-pressure fluctuations*, NASA Contractor Report 198276, NASA, 1996.

A.V. Smol'yakov and V.M. Tkachenko, *Model of a field of pseudosonic turbulent wall pressures and experimental data*, Soviet Physics - Acoustics 37(6), pages 627–631, 1991.

S. Song, D.B. DeGraaff and J.K. Eaton, *Experimental study of a separating, reattaching, and redeveloping flow over a smoothly contoured ramp*, International Journal of Heat and Fluid Flow 21, pages 512–519, 2000.

H. Stüer, A. Gyr and W. Kinzelbach, *Laminar separation on a forward facing step*, European Journal of Mechanics B/Fluids 18, pages 675–692, 1999.

W.W. Willmarth, *Pressure fluctuations beneath turbulent boundary layers*, Annual Review of Fluid Mechanics 7, pages 13-38, 1975.

S.F. Wu and L. Maestrello, *Responses of finite baffled plate to turbulent flow excitations*, AIAA Journal 33, pages 13–19, 1995.